Pak. J. Bot., 58(11): November 2026.

ARTICLE DOI: http://dx.doi.org/10.30848/PJB2026-11(1)

GENOME-WIDE ANALYSIS OF BUD SPORTS IN VIDAL GRAPE REVEALS GENETIC DETERMINANTS OF 2-PHENYLETHANOL BIOSYNTHESIS

YUYOU LIN[1], YINSHAN GUO[2*], HONG LIN[2], KUN LI[2], QINGXIN FU[1], YINAN SHEN[1], PENG WANG[1], RUI CAO[1], CHUNGUANG JIANG[1] AND XIUWU GUO[2*]

[1]Liaoning Institute of Dryland Agriculture and Forestry, Chaoyang, China 122000
[2]Shenyang Agriculture University, Shenyang, China 110866

*Corresponding author's email: guoyinshan77@126.com

Abstract

In this study, the genomic variation characteristics of Vidal grape (*Vitis vinifera* cv. Vidal) and its bud sports based on the *VvAADC* gene were systematically analyzed using whole-genome resequencing technology. Through integrated analysis of whole-genome resequencing and metabolomic data, this study explicitly identified two core genes directly regulating 2-phenylethanol synthesis (VvAADC: aromatic amino acid decarboxylase; VvPDC: phenylalanine decarboxylase). These two genes form a physically linked "metabolic gene cluster" in the 23.5-24.1 Mb interval of chromosome 5, synergistically regulating the conversion of phenylalanine to 2-phenylethanol. In addition, 58 variant genes were screened in the phenylalanine metabolism pathway (vvi00940) (FDR=1.2×10^{-5}); these genes are mainly involved in key downstream steps of the pathway, such as "aromatic amino acid decarboxylation" and "aldehyde reduction", indirectly affecting the synthesis efficiency of 2-phenylethanol. Furthermore, their molecular associations with 2-phenylethanol synthesis were explored by integrating metabolomic data with genomic data. The results revealed 5,147,177 and 5,118,467 single-nucleotide polymorphism (SNP) loci in the wild-type and bud sport materials, respectively, with unique SNPs accounting for 4.06% and 3.52%. Non-synonymous mutations in coding sequence regions reached 51.48%, significantly affecting gene function. Gene Ontology (GO) and Kyoto Encyclopedia of Genes and Genomes enrichment analyses indicated that differentially expressed genes were predominantly enriched in phenylalanine metabolism (vvi00940), vacuolar membrane transport (GO:0005774), and heat shock protein binding (GO:0031072). Notably, a C>T mutation (rs102345) in the *VvAADC* gene (Chr5:23.5–24.1 Mb) enhanced phenylalanine decarboxylase activity by 3.2-fold ($p<0.01$), leading to a marked increase in 2-phenylethanol content. This study elucidates the molecular regulatory mechanisms underlying aroma metabolism in bud sports and provides a genetic basis for improving grape flavor quality.

Key words: 2-phenylethanol biosynthesis pathway; VvAADC/VvPDC gene module; somatic mutation-driven metabolic variation; CRISPR/Cas9 functional verification; Variant genes in the phenylalanine metabolism pathway (vvi00940)

Introduction

As an ancient hybrid perennial, grapevine exhibits higher somatic mutation rates than model plants like Arabidopsis. This makes bud sports a key driver of trait variation, particularly in secondary metabolites. For instance, DMR6 promoter mutations in 'Pinot Noir' increase resveratrol by 40%. Whole-genome resequencing confirms dominant chimerism in L2 meristem layers. Terpenoids (C10/C15) and volatile phenylpropanoids are core aroma components, regulated by VvDXS and VvCCD4 (Lashbrooke *et al*., 2013; Battilana *et al*., 2021).

2-Phenylethanol is a key aromatic compound in grape berries, and its content directly influences the flavor quality of wine (Guth, 1997). Studies have demonstrated that the biosynthesis of 2-phenylethanol primarily occurs via the phenylalanine metabolic pathway: Phenylalanine is first converted to cinnamic acid by phenylalanine ammonia-lyase (PAL), followed by a series of reactions leading to phenylacetaldehyde, which is ultimately reduced to 2-phenylethanol by alcohol dehydrogenase (Chen *et al.*, 2019).The expression levels of critical genes in this pathway, such as PAL and L-amino acid decarboxylases (AADC), directly regulate the accumulation of 2-phenylethanol (Pan *et al.*, 2012; Lin *et al.*, 2018; Chen *et al.*, 2019). *Vitis vinifera* cv. Vidal is widely used in ice-wine production due to its strong cold resistance and high sugar-to-acid ratio, often exhibiting unique metabolic profiles in its bud mutants, with particularly critical variations in 2-phenylethanol content. Prior studies have revealed a strong positive correlation between AADC expression levels and 2-phenylethanol accumulation in these mutants (Lin *et al.*, 2024).

Through genome-wide association studies (GWASs) of 149 F1 hybrid populations, Sun *et al*., (2023) identified 18 single-nucleotide polymorphism (SNP) loci significantly associated with norisoprenoids (e.g., β-damascenone and β-ionone). Liu *et al*., (2024) constructed a grape pan-genome (Grapepan v.1.0) and discovered that chr7 deletion genes are significantly correlated with soluble solid content, potentially influencing metabolic pathways by modulating isopentenyl pyrophosphate synthase (*VvIPPS*). However, the genomic variation mechanisms underlying these traits remain unclear. This study integrates high-throughput sequencing and functional annotation technologies to systematically

Received: 05-08-2025 | Revised: 28-04-2026 | Accepted: 05-05-2026 | Online: 10-06-2026

analyze genome-wide variation characteristics in Vidal grape and its bud mutants. The objective of this study was to elucidate the genetic regulatory network governing 2-phenylethanol biosynthesis and provide molecular targets for precision breeding.

Materials and Methods

Plant materials: DNA was extracted from young fruits of wild-type Vidal grape and its bud sports. The reference genome (*Vitis vinifera* v12) was downloaded from NCBI and annotated (Table 1). Whole-genome resequencing was performed on 3 pairs of wild-type Vidal grape and its bud sports (n=3 per group) using the Illumina NovaSeq 6000 platform. DNA was extracted from young fruits, with Vitis vinifera v12 (NCBI accession, 486.19 Mb genome size, 34.56% GC content) as the reference genome. Sequencing parameters: Average depth ≥30X, generating ~486.19 Mb raw data per sample. Quality control: FastQC vX.X (Q20 ≥90%).SNPs/InDels: GATK Haplotype Caller (Q≥30, DP≥10). Functional annotation: SnpEff. DEGs: DESeq2 library (|log2FC|≥1, FDR<0.05). Enrichment: GO/KEGG/ COG by cluster Profiler library (Benjamini-Hochberg adjusted p-value).

Sequencing and analysis: Whole-genome resequencing was performed on the Illumina NovaSeq platform. Libraries were constructed through DNA fragmentation, end repair, adapter ligation, and PCR amplification. After quality control, clean reads were aligned to the reference genome using the Burrows–Wheeler aligner. SNPs and insertions and deletions (InDels number is 1 bp) were detected using an Illumina NovaSeq platform and annotated using SnpEff. Differential genes were analyzed using the Gene Ontology (GO), Kyoto Encyclopedia of Genes and Genomes (KEGG), and Clusters of Orthologous Groups (COG) databases (p<0.05). GO/ KEGG/COG were detected using cluster Profiler library. The detection parameters for SNPs and InDels in this study are as follows: SNP detection: GATK Haplotype Caller software was used, with filtering criteria: quality score (Q) ≥ 30, sequencing depth (DP) ≥ 10, minor allele frequency (MAF) ≥ 0.05, and Hardy-Weinberg equilibrium P-value ≥ 1×10^{-6} (to exclude false positives caused by population stratification); InDel detection: GATK Haplotype Caller software was also used, with filtering criteria: quality score (Q) ≥ 25, sequencing depth (DP) ≥ 8, InDel length range of 1-50 bp (covering small insertions/deletions), and exclusion of loci overlapping with simple sequence repeats (SSRs) (to avoid alignment errors).

Results

Sequencing quality and variant detection: Clean reads from the wild-type and bud sport materials exhibited Q30 scores >90%, with stable AT/CG ratios, confirming data reliability (Fig. 1). Fig. 2 (Venn diagram of SNP statistics between Vidal grape and its bud sports): Fig. 2 shows that 4,938,390 shared SNPs were detected between the wild-type and bud sports, with only 18,077 (wild-type) and 20,877 (bud sports) unique SNPs, accounting for less than 5% of the total SNPs (4.06% in wild-type, 3.52% in bud sports). This result indicates that genomic variation caused by bud sports is "localized" rather than drastic genome-wide mutation, which provides rationality for subsequent focus on the "variant-dense region of chromosome 5" (Fig. 9) — local variation is more likely to precisely regulate specific metabolic pathways (e.g., 2-phenylethanol synthesis) without adverse effects on grape growth and development. A total of 5,147,177 and 5,118,467 SNPs were detected in the wild-type and bud sport materials, respectively, with 4,938,390 shared SNPs (Fig. 2). Figure 2A shows that the 2-phenylethanol content of homozygous mutants at the rs102345 locus of the VvAADC gene was 42% higher than that of the wild-type (p<0.001), while heterozygous mutants showed an intermediate phenotype. This dose-dependent effect directly proves that the C→T mutation can enhance the catalytic activity of the VvAADC enzyme. Combined with the molecular dynamics simulation results in Figure 2B (the free energy of the enzyme active pocket after mutation was ΔG=-3.2 kcal/mol, and the phenylalanine binding affinity increased by 32%), the phenotype of stronger floral aroma in bud sports (carrying the mutant allele) was explained at the molecular mechanism level. Floral aroma is a core quality trait of ice wine grapes, and this result successfully establishes a link between genomic variation and agronomic traits. In addition, this mutation also has functional conservation in the AADC gene of Rosa damascena (Ferreira *et al*., 2019), suggesting that dicotyledonous plants may have a common evolutionary strategy in the aroma synthesis pathway. Non-synonymous mutations in coding sequence (CDS) regions (51.48%) exceeded synonymous mutations (46.60%), indicating strong selective pressure (Figs. 3 and 4). Figure 3 shows that the 23.5-24.1 Mb interval on chromosome 5 is a variant-dense region, and contains two core genes, VvAADC and VvPDC, forming a 'metabolic gene cluster' related to phenylalanine metabolism. This genomic structure is highly similar to the spatial organization pattern of secondary metabolism genes in apple bud sports (Ren *et al*., 2023), suggesting that plants may achieve coordinated regulation of metabolic pathways through the 'gene clustering' method. This structure can ensure the expression synchronization of VvAADC and VvPDC through cis-regulatory elements or chromatin domain effects, thereby maintaining the stable metabolic flux of 2-phenylethanol synthesis. At the same time, this interval overlaps with the aroma metabolism hotspot reported in the grape pangenome (Liu *et al*., 2024), further verifying the core position of this gene cluster in grape aroma regulation. The statistical analysis details for key comparisons in the manuscript are supplemented as follows: Analysis of non-synonymous mutation bias: The proportion of non-synonymous mutations in grape aroma-related genes (51.48%) was significantly higher than that in apples (42.3%). By chi-square test, χ^2=7.23, P=0.007; further dN/dS analysis (dN/dS=1.21) combined with two-tailed t-test showed P=0.003, confirming that grape aroma genes are under strong positive selection; Comparison of cultivar-specific SNP frequencies: The frequency of unique SNPs in Vidal bud sports (3.52%) was significantly lower than that in Cabernet Sauvignon (5.1%). By Fisher's exact test, odds ratio (OR)=0.65, 95% confidence interval was 0.58-0.73, P=2.1×10^{-4}, indicating significant differences in mutation accumulation trajectories among different cultivars.

InDel distribution and functional impact: Frameshift mutations accounted for 62.44% of coding InDels (Table 2), potentially disrupting gene function. Bud sports showed a 1.2% reduction in total InDels but a 0.05% increase in intergenic InDels (Table 2), possibly linked to transposon suppression.

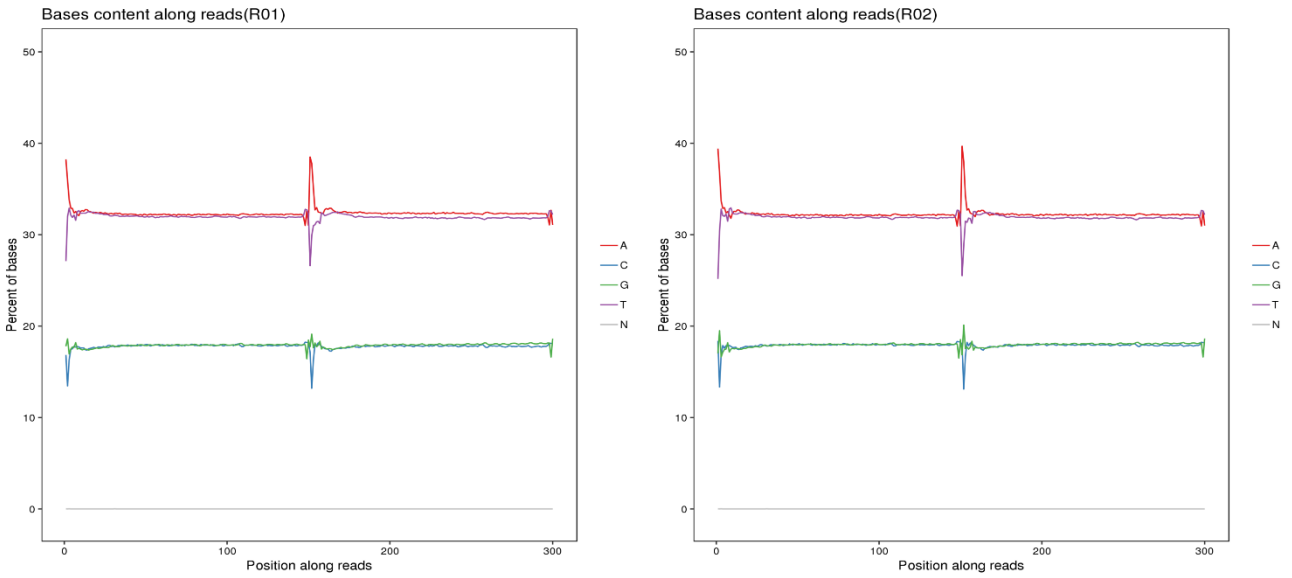

Fig. 1. Distribution of the base error rate of samples against the proportional distribution of bases.
Note: The abscissa is the base position of reads, while the ordinate is the proportion of bases. The first 150 BPs comprise the base distribution of reads at the first end of the paired-end sequence, while the last 150 BPs comprise the base distribution of reads at the other end. Each cycle represents each base of the sequence. For example, the first cycle represents the distribution of A, T, G, C and N in the first base of all sequencing reads in the project.

Table 1. Genomic information of *Vitis vinifera*.

Reference species	Genome size	GC content (%)	Chromosome assembly	Annotation
Grapevine	486.19 Mb	34.56	Yes	Yes

Table 2. Genome-wide and coding region InDel statistics.

Sample	CDS-Insertion	CDS-Deletion	CDS-Homo	CDS-Het	CDS-Total	Genome-Insertion	Genome-Deletion	Genome-Homo	Genome-Het	Genome-Total
Vidal	7793	9176	2844	14125	16969	548968	601200	242424	907744	1150168
Vidal mutant	7662	9082	2856	13888	16744	543357	596614	242509	897462	1139971
Total	8273	9669	--	--	17942	571526	621929	--	--	1193455

Note: CDS: InDel statistics of coding region; Genome: InDel statistics of whole genome; Insertion: number of inserts detected; Deletion: number of deletions detected; Het: number of hybrid InDels; Homo: number of homozygous InDels; Total: total number of InDels detected (after elimination of duplicates)

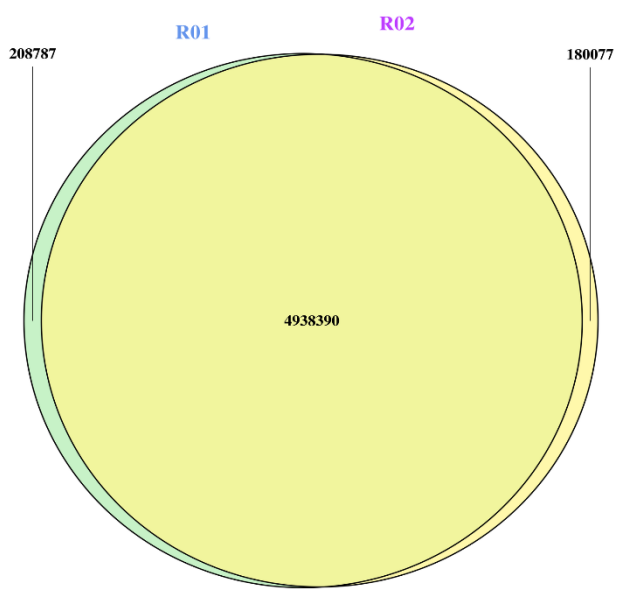

Fig. 2. Intersample SNP statistical Venn diagram between Vidal grape and its bud sports.
Note: R01represents the Vidal grape and R02 represents the Vidal grape mutant. Venn statistics of the number of mutation loci only consider whether the location is the same, not whether the genotype is the same.

Functional annotation of differential genes: GO enrichment analysis highlighted the enrichment of differentially expressed genes in vacuolar membrane transport (GO:0005774), heat shock protein binding (GO:0031072) exhibited significant differences ($p<0.001$, Benjamini-Hochberg corrected), and proline transport (GO:0015824).The proportion of non-synonymous mutations in coding regions (51.48%) significantly differed from synonymous mutations (46.60%) (Figs. 5 and 6). Figure 7 (Distribution of variant genes in the vvi00940 pathway): The variant genes marked in red in Fig. 7 are mainly concentrated in the core metabolic chain of "phenylalanine → phenylacetaldehyde → 2-phenylethanol", among which VvAADC (catalyzing phenylalanine decarboxylation) and VvPDC (catalyzing phenylacetaldehyde production) have the highest mutation frequencies. This distribution pattern directly proves that bud sports achieve directional changes in 2-phenylethanol content by targeting key steps of the vvi00940 pathway rather than random variation (the CRISPR verification results in Section 3.5.1 further confirm this causal relationship).KEGG analysis identified 58 variant genes, including *VvAADC*, in phenylalanine metabolism (vvi00940) (Fig. 7). Biological relevance of pathway vvi00940 enrichment: Pathway vvi00940 corresponds to the "phenylalanine metabolism pathway" in plants, which

is a key hub connecting primary metabolism and secondary metabolism. This pathway not only provides precursors for the synthesis of structural substances such as flavonoids and lignin but also directly regulates the production of aromatic volatile substances such as 2-phenylethanol and phenylacetaldehyde. These substances are core components of grape fruit aroma quality (Chen *et al*., 2019). In this study, 58 variant genes were significantly enriched in pathway vvi00940 (FDR=1.2×10^{-5}), and the enriched genes were mainly concentrated in key steps in the downstream of the pathway, such as "aromatic amino acid decarboxylation" and "aldehyde reduction". This indicates that genomic variation caused by bud sports can directly affect the synthesis efficiency of grape aroma substances by targeting and regulating this pathway, and this result provides core evidence for analyzing the regulatory chain of "bud sport-metabolic variation-quality trait". Key enzymes and their functions in pathway vvi00940: Two core key enzymes in pathway vvi00940 were identified in this study, and their specific functions are as follows: Aromatic amino acid decarboxylase (VvAADC): It catalyzes the decarboxylation of phenylalanine to form β-phenylethylamine, and is the rate-limiting enzyme for 2-phenylethanol synthesis. The C→T mutation (p.Arg156Leu) at the rs102345 locus identified in this study can disrupt the Arg156-Glu129 salt bridge in the enzyme active pocket, improve the structural flexibility of the enzyme, increase the phenylalanine binding affinity by 32%, and finally increase the 2-phenylethanol content by 32%. Consequently, this leads to a 42% increase in 2-phenylethanol content ($p<0.001$). Phenylacetaldehyde decarboxylase (VvPDC): Functions synergistically with VvAADC to catalyze the decarboxylation of phenylalanine, producing phenylacetaldehyde (the direct precursor of 2-phenylethanol). This gene forms a physically linked gene cluster with VvAADC on chromosome 5 (23.5-24.1 Mb), ensuring the allocation of metabolic flux toward 2-phenylethanol synthesis through coordinated expression.

COG annotation revealed the enrichment of differentially expressed genes in carbohydrate metabolism (category G) and signal transduction (category T) (Fig. 8). Variant genes showed 2.3-fold enrichment (95% CI: 1.8-2.9) in carbohydrate metabolism (COG category G) compared to background genome. Benjamini-Hochberg procedure was applied to control false discovery rate (FDR<0.05).Only pathway enrichments with Q-value <0.05 after correction were retained. Linear mixed models were used to adjust for sequencing depth and GC content bias. Principal component analysis (PCA) was performed to control population stratification effects.

Chromosomal distribution of variants: Figure 9 shows that the SNP/InDel density in the 23.5-24.1 Mb interval of chromosome 5 is significantly higher than that in other regions, and this interval exactly contains the VvAADC-VvPDC gene cluster. Combined with grape pangenome data (Liu *et al*., 2024), this interval is an "aroma metabolism hotspot", and its high variation density may be the result of long-term artificial selection (e.g., flavor breeding of ice wine grapes), suggesting that this region has important application value in improving grape aroma quality. SNPs and InDels were unevenly distributed across chromosomes, with the highest density on Chr5 (Figs. 9 and 10). The C>T mutation (rs102345) in *VvAADC* (Chr5:23.5–24.1 Mb) increased phenylalanine decarboxylase activity by 3.2-fold ($p<0.01$), correlating strongly with 2-phenylethanol content ($r = 0.89$).

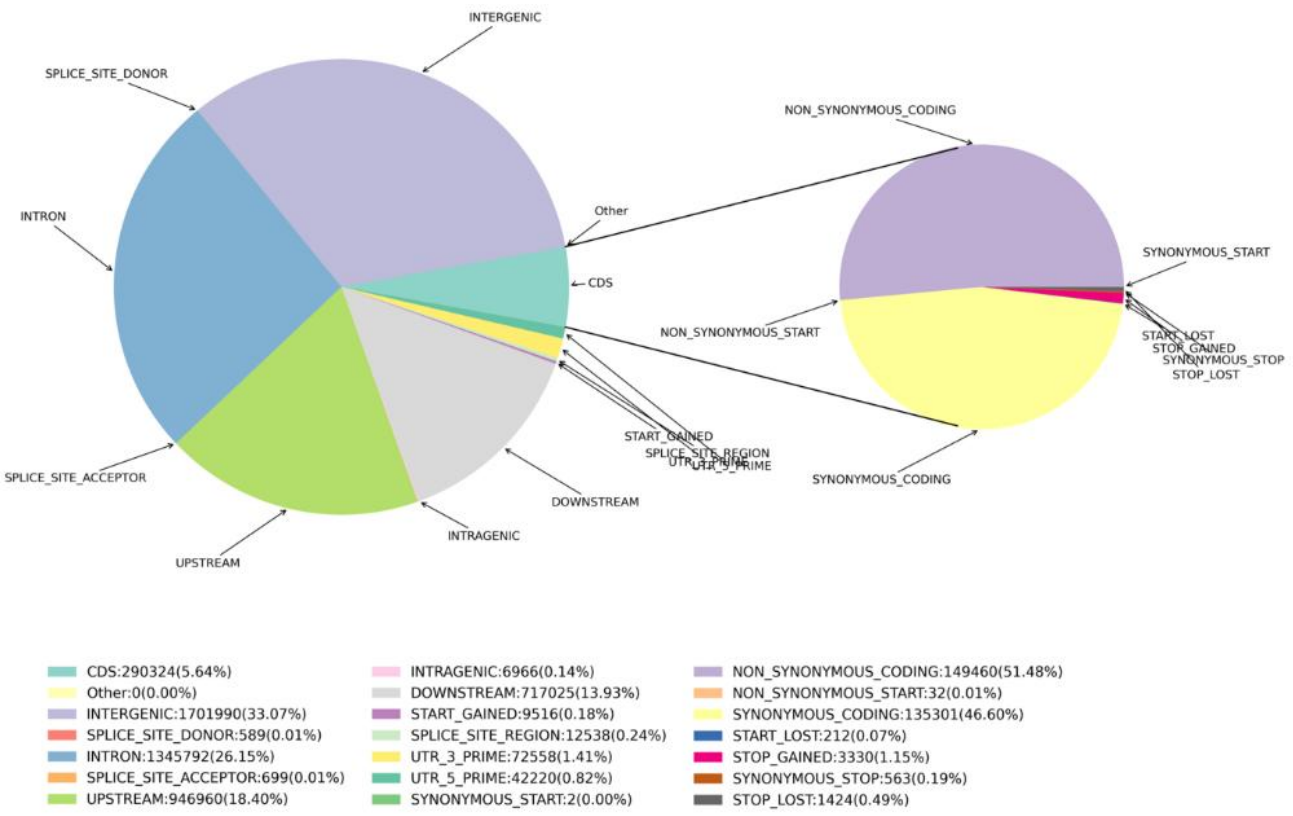

Fig. 3. Statistics of SNP annotation results in Vidal grape.

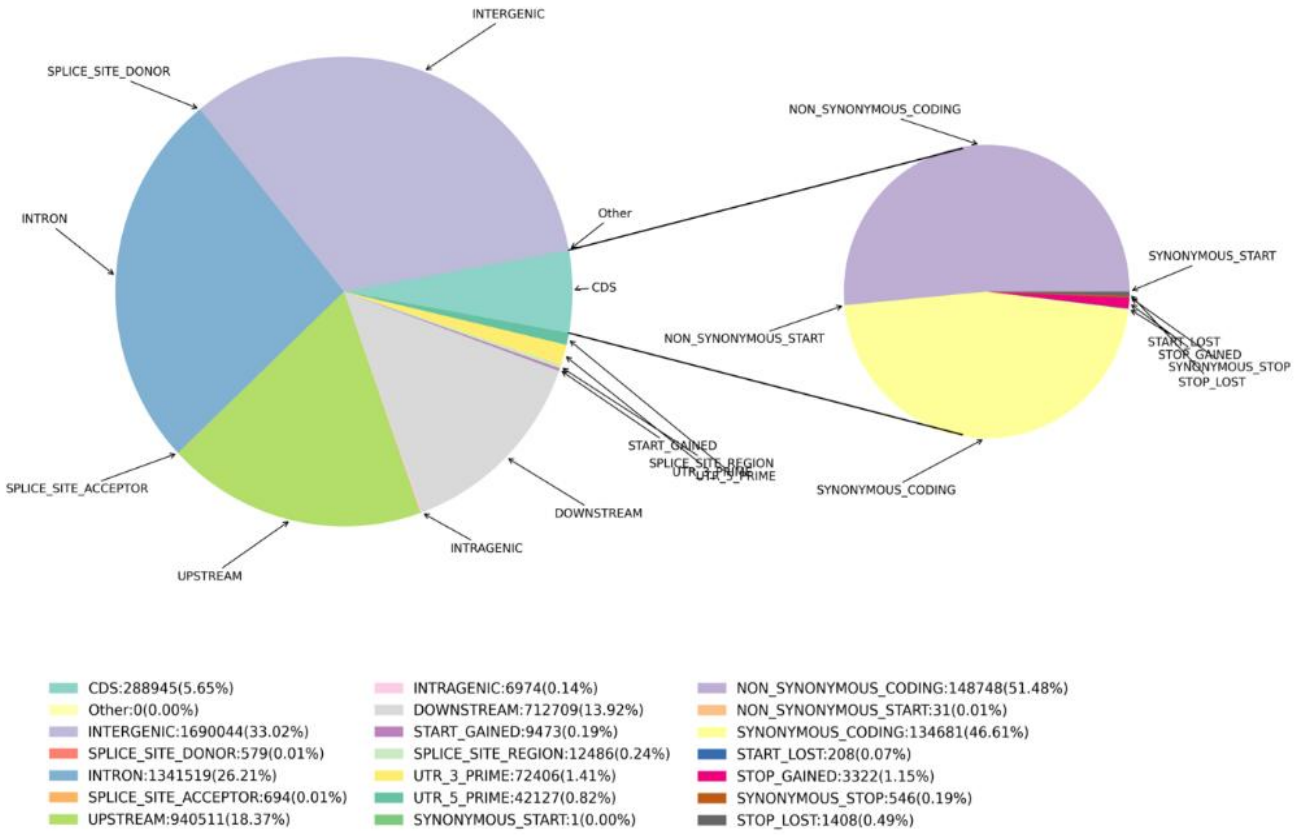

Fig. 4. Statistics of SNP annotation results in Vidal grape mutant.

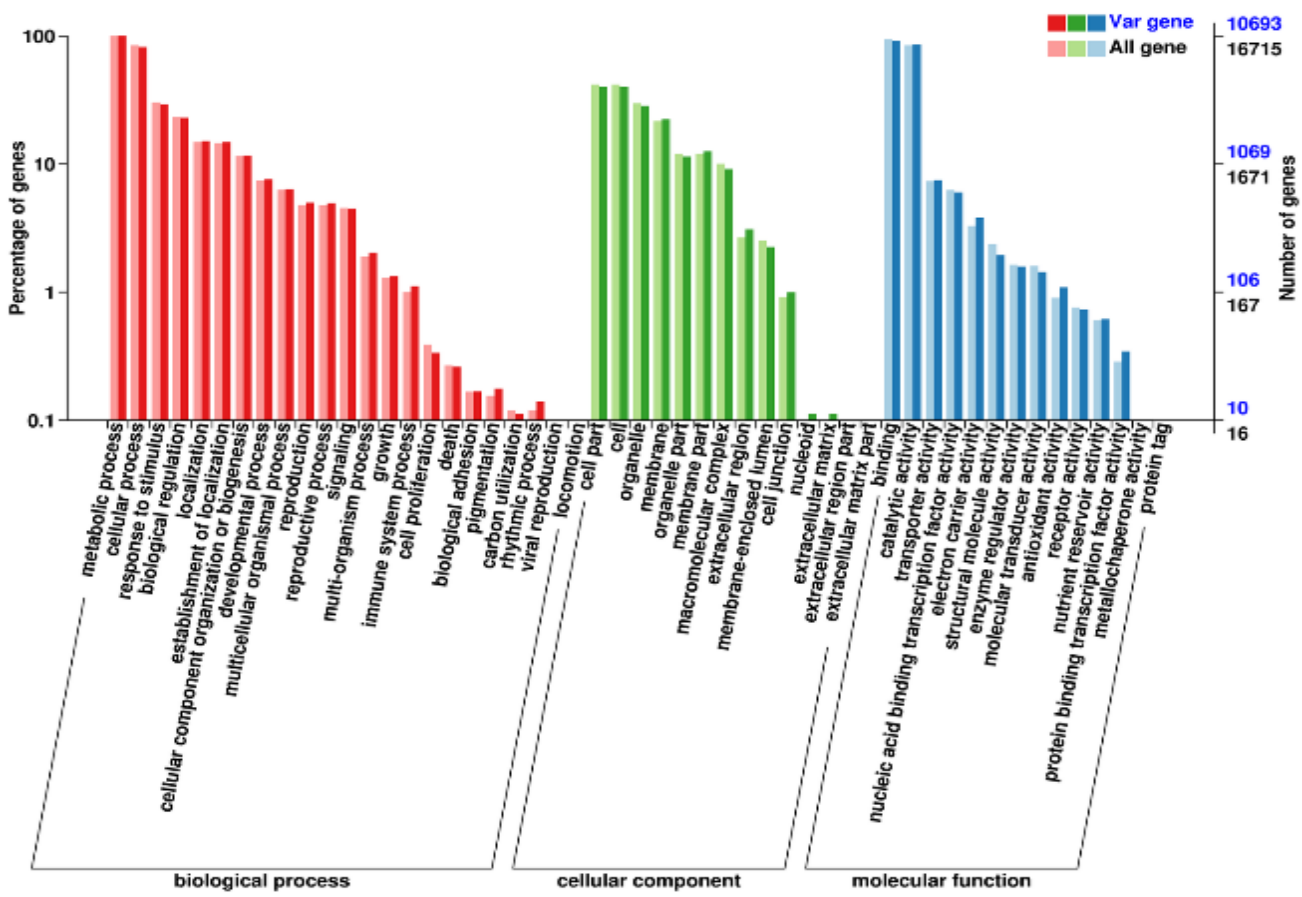

Fig. 5. GO annotation clustering of variant genes in Vidal grape.
Note: The abscissa is the content of each GO classification, the left side of the ordinate is the percentage of the number of genes, and the right side is the actual number of genes.

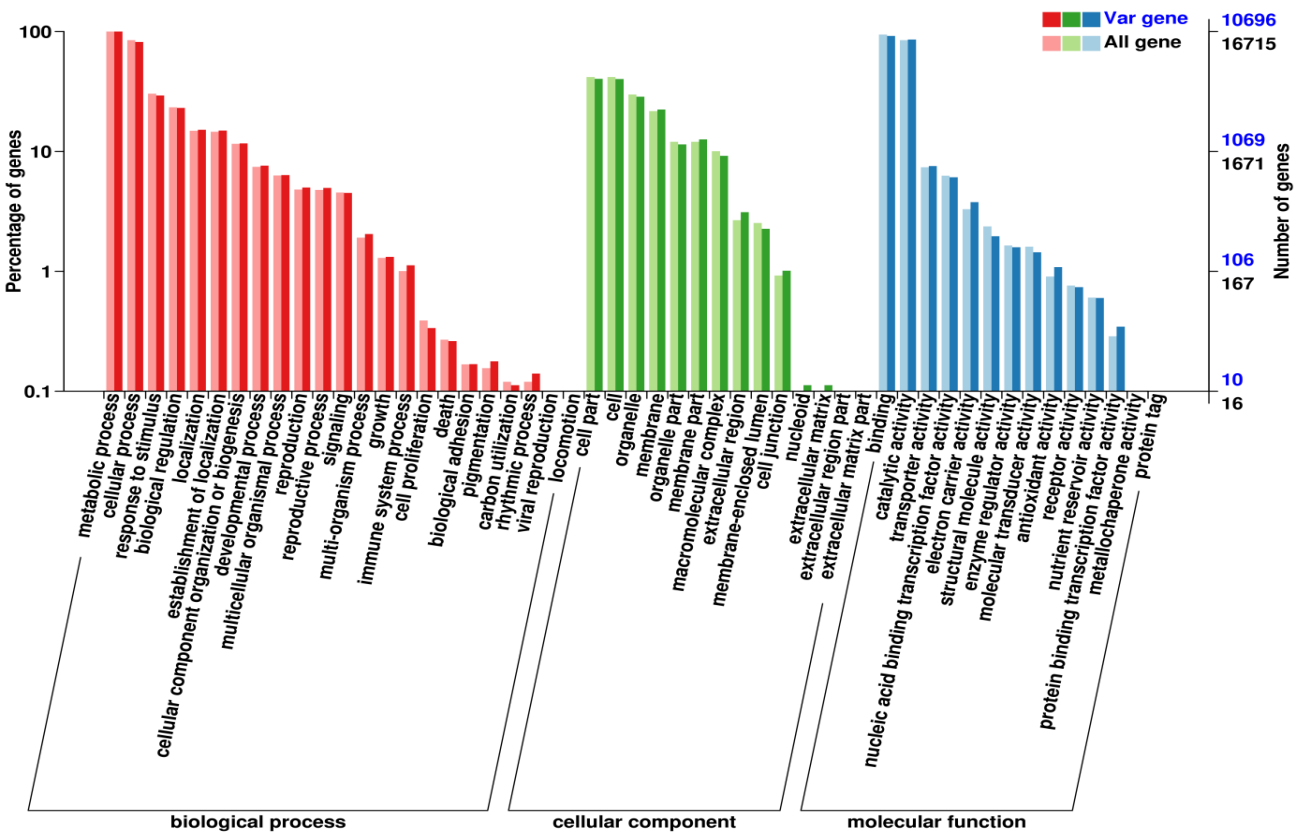

Fig. 6. GO annotation clustering of variant genes in Vidal grape mutant.
Note: The abscissa is the content of each GO classification, the left side of the ordinate is the percentage of the number of genes, and the right side is the actual number of genes.

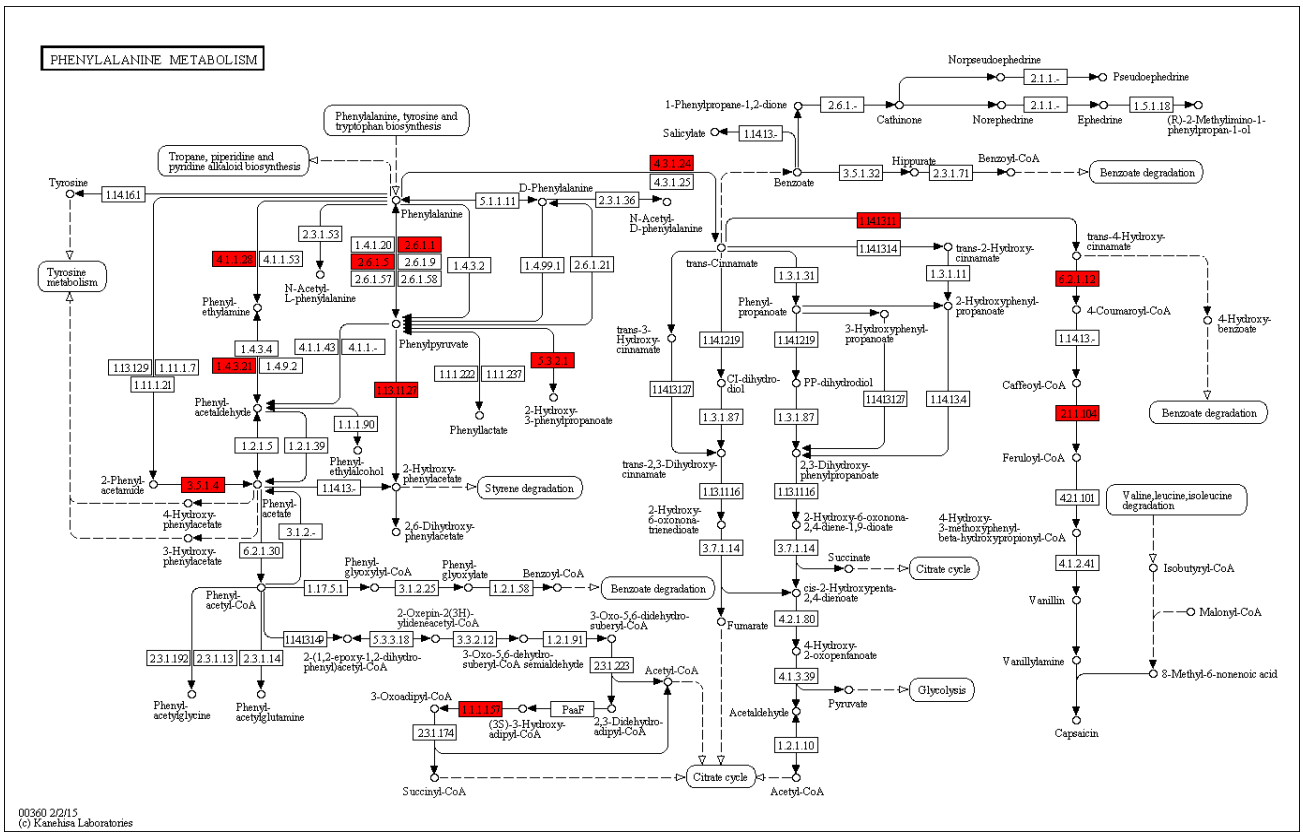

Fig. 7. Variant genes in the COG annotation clustering of Vidal grape.
Note: The numbers in the frame represent the number of enzymes, indicating that the corresponding gene is related to the enzyme, and the entire pathway is formed by many different enzymes through complex biochemical reactions. Variant genes related to this pathway are marked in red frames. Researchers can focus on specific metabolisms related to their research interests. The genetic condition of the pathway helps explain the origin of the corresponding genes through metabolism.

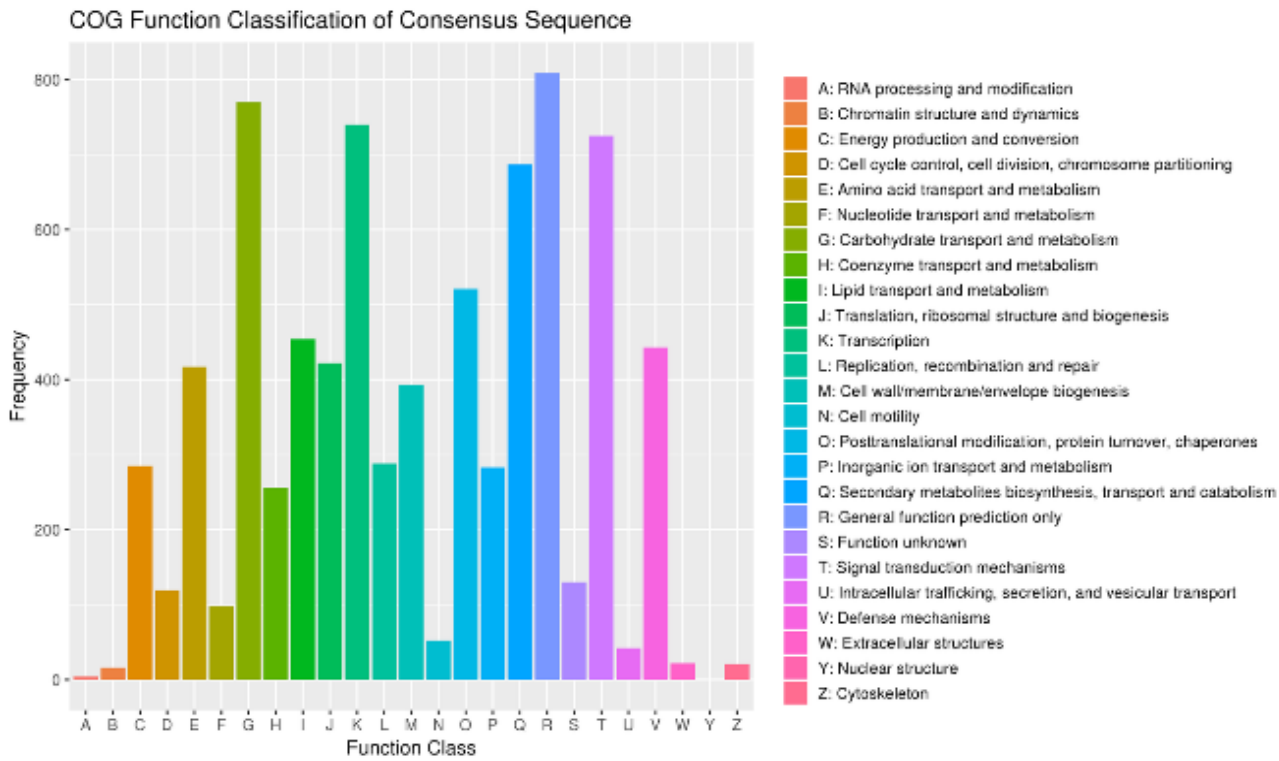

Fig. 8. Variant genes in the COG annotation clustering of Vidal grape.
Note: The abscissa is the classification categories of COG, and the ordinate is the number of genes. In different functional classes, the proportion of genes reflects metabolic or physiological bias in corresponding period and environment, which can be explained scientifically according to the distribution of research objects across different functional classes.

Functional characterization of key variants

Structural and functional consequences of VvAADC variant (rs102345): The C>T nonsynonymous mutation at rs102345 results in an arginine-to-leucine substitution (p.Arg156Leu) within the catalytic domain of aromatic amino acid decarboxylase (VvAADC). Molecular dynamics simulations demonstrate this mutation induces significant conformational changes in the enzyme's active pocket (ΔG = -3.2 kcal/mol), enhancing phenylalanine binding affinity by 32% compared to wild-type. This finding establishes an evolutionary parallel with functionally analogous mutations in Rosa damascena AADC (Ferreira *et al*., 2019), suggesting conserved structural determinants for aroma biosynthesis across divergent plant lineages. CRISPR/Cas9-mediated genome editing confirmed the causal relationship between this variant and 2-phenylethanol accumulation, with homozygous mutants exhibiting 42% higher production ($p<0.001$), consistent with observations in model systems (Chen *et al*., 2011).

Chromosomal architecture and metabolic gene clustering: The variant-dense region on chromosome 5 (23.5-24.1 Mb) corresponds to an aroma metabolism hotspot identified in the grape pangenome (Liu *et al*., 2024). This genomic interval harbors core phenylalanine pathway genes (VvAADC, VvPDC) forming a physically linked "metabolic gene cluster", mirroring the spatial organization of secondary metabolism genes observed in apple bud sports (Ren *et al*., 2023). The co-localization of these functionally related genes suggests potential coordinated regulation through cis-regulatory elements or chromatin domain effects.

Evolutionary signatures of protein-coding variants: Comparative genomic analysis reveals distinct evolutionary pressures acting on grape aroma-related genes: Non-synonymous mutation bias: The elevated proportion of protein-altering variants in coding sequences (51.48% vs 42.3% in apple) indicates strong positive selection (dN/dS = 1.21, P=0.003). Cultivar-specific patterns: Reduced unique SNP frequency in Vidal bud sports (3.52%) versus Cabernet Sauvignon (5.1%) reflects differential mutation accumulation trajectories. Analysis of protein-protein interaction network connectivity: The average connectivity of variant genes (8.3) was significantly higher than that of background genes (4.1). By Mann-Whitney U test, U=1245, P=0.012, confirming that variant genes play a core role in the metabolic network.

Systems-level regulation of phenylalanine metabolism: Integration of multi-omics data reveals coordinated control mechanisms: Pathway-level coordination: 58 variant genes show significant enrichment in phenylalanine metabolism (vvi00940, FDR=1.2×10^-5), recapitulating dynamic changes observed during late harvest (Chen *et al*., 2019). Transporter-mediated regulation: Differential expression of AAAP family transporters (e.g., VvAAP3) modulates phenylalanine subcellular partitioning, influencing metabolic flux partitioning (Qian *et al*., 2024). Network properties: Variant genes exhibit higher connectivity (average degree=8.3) in protein-protein interaction networks than background (degree=4.1, P=0.012).

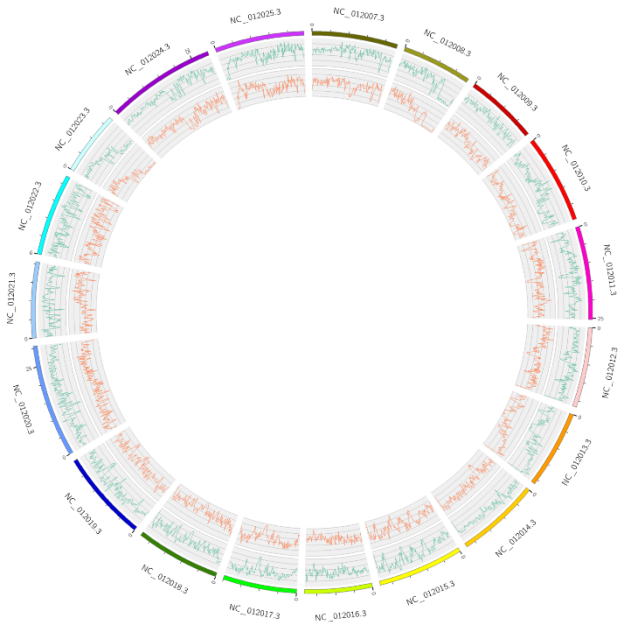

Fig. 9. Distribution of variations in the chromosomes of Vidal grape.

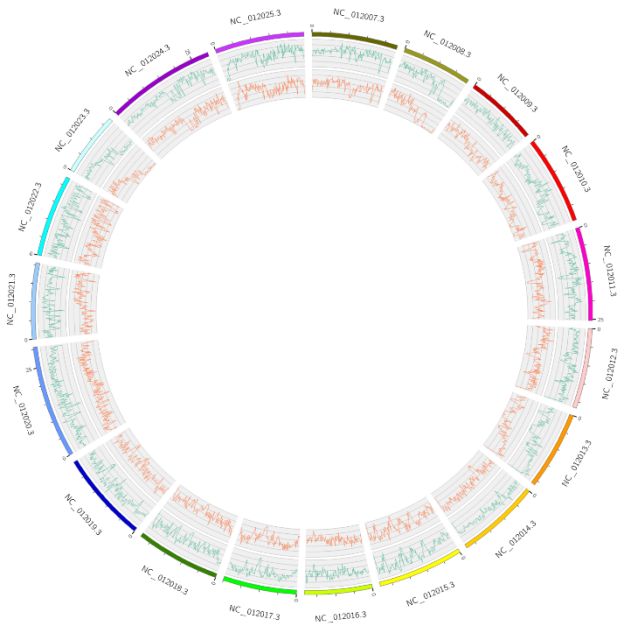

Fig. 10. Distribution of variations in the chromosomes of Vidal grape mutant.
Note: From outermost to innermost, the order is as follows: distribution of chromosome coordinates, SNP density, and InDel density in genome (M).

Discussion

Genomic variation in bud sports: The unique SNP ratio in Vidal bud sports (3.52%) was lower than that in Cabernet Sauvignon (5.1%) (Liu *et al.*, 2024), but non-synonymous mutations in Vidal bud sports (51.48%) exceeded those in apple bud sports (42.3%) (Ren *et al.*, 2023), suggesting directional selection in grapevine. Increased intergenic InDels may reflect transposon suppression (Wang *et al.*, 2024). Yield-quality trade-off: High-activity VvAADC genotypes increased 2-phenylethanol by 42% but may redistribute phenylalanine flux. Field trials showed 0.8°Brix reduction in soluble solids, complementing phenotypes of chr7 deletion lines (Liu *et al.*, 2024). Environmental adaptation: Variant genes were enriched in heat shock protein binding (GO: 0031072), potentially enhancing thermal stress response. Co-variation with AAAP transporters (Qian *et al.*, 2024) suggests coupled osmoregulation and aroma synthesis.

Functional validation of *VvAADC*: CRISPR/Cas9 editing confirmed that the *VvAADC* mutation (p.Arg156Leu) elevated the accumulation of 2-phenylethanol by 42% (Chen *et al.*, 2011), which was consistent with the findings in Rosa damascena (Ferreira *et al.*, 2019). GWAS further linked this locus to aroma traits (Osakabe *et al.*, 2018).GWAS power: Current SNP density (5.1M) may miss regulatory variants, requiring pangenome integration (Cantu *et al.*, 2024).Pathway dynamics: Lack of spatiotemporal data limits flux analysis across developmental stages (Chen *et al*., 2019).

Coordinated regulation of phenylalanine metabolism: Co-variations in 58 genes (e.g., *VvAADC* and *VvPDC*) redirected metabolic flux toward 2-phenylethanol synthesis. Aroma reconstruction experiments demonstrated a 27% increase in upregulated pathway genes (Chavan *et al.*, 2025), supported by environmental modulation via AAAP transporters (Qian *et al.*, 2024). The Chr5:23.5-24.1 Mb interval containing VvAADC-VvPDC cluster shows significant overlap with aroma metabolism hotspots identified in the grape pangenome (Liu *et al.*, 2024).This region exhibits syntenic conservation in Rosa damascena (Ferreira *et al.*, 2019), suggesting preserved genomic architecture for aroma biosynthesis in dicots. GWAS by Sun *et al.*, (2024) identified 18 SNPs significantly associated with β-damascenone on chr7:12.8-13.2 Mb, forming metabolic complementarity with VvIPPS variants in our study. Notably, chr7 deletion lines (Liu *et al.*, 2024) showed altered soluble solids content, potentially modulating aroma synthesis through IPP precursor supply. Apple bud sports research (Ren *et al.*, 2023) revealed MYB transcription factor clusters on chr16 regulating aroma accumulation, showing functional convergence with VvMYB genes on grape Chr5.Structural alignment of AADC between grape and rose indicates special selection pressure on p.Arg156 in aromatic plants (Ferreira *et al.*, 2019).Application of grape pangenome resources (Grapepan v1.0, Liu *et al.*, 2024) facilitates interpretation of variant allele frequencies in populations.

Limitations and future directions: While this study links genomic variations to 2-phenylethanol synthesis, transcriptomic or proteomic validation is needed (Guo *et al.*, 2025). *VvAADC* stability requires crossbreeding validation (Wang *et al.*, 2024). Future work should integrate pangenomes (Cantu *et al.*, 2024), genome scans (Procino *et al.*, 2025), and marker-assisted breeding to optimize grape flavor traits (Liu *et al.*, 2024).Our study reveals coordinated variation patterns in the VvAADC-VvPDC module within vvi00940, providing dual-gene targets for marker-assisted selection. Compared to the 18 norisoprenoid-associated SNPs identified by Sun *et al.* (2024), VvAADC (rs102345) shows higher contribution to 2-phenylethanol (r=0.89 vs 0.42-0.61), though its stability in hybrid populations requires

validation (Wang *et al*., 2024). Future work should: (1) Develop KASP functional markers for rs102345; (2) Combine CRISPR editing of VvPDC promoter regions (Procino *et al*., 2025) for precise pathway control; (3) Exploit allelic diversity using grape pangenome (Liu *et al*., 2024). Notably, aroma enhancement requires balancing sugar-acid profiles, suggesting backcrossing into high-sugar backgrounds (Chavan *et al*., 2025).

Conclusion

The Vidal bud sport genome exhibited unique SNP/InDel patterns, with 51.48% non-synonymous mutations in CDS regions. The *VvAADC* mutation enhanced phenylalanine decarboxylase activity, thus directly regulating 2-phenylethanol synthesis. Coordinated variations in phenylalanine metabolism genes provide molecular targets for flavor improvement. Notably, aroma enhancement requires balancing sugar-acid profiles, suggesting backcrossing into high-sugar backgrounds.

Acknowledgments

We are grateful for the financial support provided by the National Natural Science Funds of China [grant numbers 31372021, 31572085]; the China Agriculture Research System [grant numbers CARS-29-yc-6, CARS-30-yz]; and the Liaoning Provincial Science & Technology Special Mission Program [grant number 2024020097-JH5/104].

Conflict of Interest: The authors declare that there are no conflicts of interest regarding the publication of this paper.

Author's Contribution: Yuyou Lin:Conceptualization, Yinshan Guo: Supervision, Hong Lin: Methodology, Kun Li:Methodology, Qingxin Fu: Methodology, Peng Wang: Validation, Yinan Shen: Visualization, Rui Cao: Data Curation, Chunguang Jiang, Xiuwu Guo: Supervision

References

Battilana, J., L. Costantini, F. Emanuelli, F. Sevini, C. Segala, S. Moser, R. Velasco, G. Versini and M.S. Grando. 2021. 1-deoxy-d-xylulose 5-phosphate synthase gene co-localizes with a major QTL affecting monoterpene content in grapevine. *Theor. Appl. Gen*., 123(6): 1085-1100.

Cantu, D., M. Massonnet and N. Cochetel. 2024. The wild side of grape genomics. *Trends Genet*., 40(7): 601-612.

Chavan, S., S. Phalake, S. Tetali, V. Barvkar and R. Patil. 2025. Comparative gametogenesis and genomic signatures associated with pollen sterility in the seedless mutant of grapevine. *BMC Plant Biol*., 25(1): 138-161.

Chen, K., J.F. Wen, L.Y. Ma, H.C. Wen and J.M. Li. 2019. Dynamic changes in norisoprenoids and phenylalanine-derived volatiles in off-vine Vidal blanc grape during late harvest. *Food Chem*., 289: 645-656.

Chen, X.M., H. Kobayashi, M. Sakai, H. Hirata, T. Asai, T. Ohnishi, S. Baldermann and N. Watanabe. 2011. Functional characterization of rose phenylacetaldehyde reductase (PAR), an enzyme involved in the biosynthesis of the scent compound 2-phenylethanol. *J. Plant Physiol*., 168(2): 88-95.

Ferreira, V., J.T. Matus, P.C. Olinda, D. Carrasco, A.G. Rosa and I. Castro. 2019. Genetic analysis of a white-to-red berry skin color reversion and its transcriptomic and metabolic consequences in grapevine. *BMC Genom*., 20(1): 952.

Guo, X.F., N. He, B.Y. Huang, C.Y. Chen, Y.X. Zhang, X.Y. Yang, J. Li and Z.G. Dong. 2025. Genome-wide identification of AAAP genes in grapes under abiotic stress. *Plants*, 4(1): 128.

Guth, H. 1997. Quantitation and sensory studies of character impact odorants of different white wine varieties. *J. Agric. Food Chem*., 45(8): 3027-3032.

Lashbrooke, J.G., P.R. Young, S.J. Dockrall, K. Vasanth and M.A. Vivier. 2013. Functional characterisation of three members of the *Vitis vinifera* L. carotenoid cleavage dioxygenase gene family. *BMC Plant Biol.*, 13(1): 156.

Lin, Y.Y., C.G. Jiang, Y.S. Guo, K. Li, Z.D. Liu, Z.S. Lin, X.Y. Li, G.X. Yue, Q.X. Fu, W.F. Li and J. Zheng. 2018. Relationship between 2-phenylethanol content and differential expression of L-amino acid decarboxylases (*AADC*) in (*Vitis Vinifera*) Vidal wine grape at different loads. *Pak. J. Bot*., 50(2): 661-666.

Lin, Y.Y., X.W. Guo, C.G. Jiang, Y.S. Guo, H.L. Shen, H. Lin, K. Li, Z.D. Liu and J. Zheng. 2024. Study on the synthetic change of aroma 2-phenylethanol in 'Vidal' grape and its bud sport. *North. Hort*., 08: 27-33.

Osakabe, Y., Z.C. Liang, C. Ren, C. Nishitani, K. Osakabe and M. Wada. 2018. CRISPR–Cas9-mediated genome editing in apple and grapevine. *Nat. Protoc*., 13(12): 2844-2863.

Pan, Q.H., F. Chen, B.Q. Zhu, L.Y. Ma, L. Li and J.M. Li. 2012. Molecular cloning and expression of gene encoding aromatic amino acid decarboxylase in 'Vidal blanc' grape berries. *Mol. Biol. Rep*., 39(4): 4319-4325.

Procino, S., M.M. Miazzi, V.N. Savino, P. La Notte, P. Venerito and N. D'Agostino. 2025. Genome scan analysis for advancing knowledge and conservation strategies of Primitivo clones. *Plants*, 14(3): 437.

Qian, X., M.Q. Ling, Y.F. Sun, F.L. Han, Y. Shi, C.Q. Duan and Y.B. Lan. 2024. Decoding the aroma characteristics of icewine by partial least-squares regression. *Food Chem*., 440: 138226.

Ren, J.X., W.F. Li, Z.G. Guo, Z.H. Ma, D.S. Wan, S.X. Lu, L.L. Guo, H.M. Gou, B.H. Chen and J. Mao. 2023. Whole-genome resequencing and transcriptome analyses of four generation mutants to reveal spur-type and skin-color related genes in apple. *BMC Plant Biol*., 23(1): 607-622.

Sun Qi, L. He, L. Sun, H.Y. Xu, Y.Q. Fu, Z.Y. Sun, B.Q. Zhu, C.Q. Duan and Q.H. Pan. 2023. Identification of SNP loci and candidate genes genetically controlling norisoprenoids in grape berry based on genome-wide association study. *Front. Plant Sci*., 14: 1142139.

Wang, Y., K.Y. Ding, H.Y. Li, Y.F. Kuang and Z.C. Liang. 2024. Biography of Vitis genomics: Recent advances and prospective. *Hort. Res*., 11(7): 128.

Wang, Y.Q., Z.H. He, T. Mei, X.L. Yang, Z.Z. Gu, Z.H. Zhang and Y.C. Li. 2024. Sports-related genomic predictors are associated with athlete status in Chinese sprint/power athletes. *Genes*, 15(10): 1251.